T.2 : Ultrafast spectroscopy of nanostructured materials

S. Khan, J. Jayabalan and Rama Chari
Laser Physics Applications Section, RRCAT, Indore
Email: chari@rrcat.gov.in

Introduction

Nanostructured materials have a great potential for a wide range of photonic devices arising from the flexibility of controlling the optical response by varying the structure [1-5]. Currently, there is a great interest in developing efficient emitters and sensors tailored for specific applications. However the various requirements for an efficient device turn out to be 'contradictory' and are not met by natural materials. A prime example is to get a strong nonlinear response which is also fast. In natural materials the strongest nonlinear response occurs near a resonance. Here the interaction cross-section is high so even with low power optical radiation it is possible to create a large excited state population and hence a strong nonlinear response. However the response time of the nonlinearity is decided by the lifetime of the excited state which is usually of the order of a nanosecond or higher. A faster response requires moving well away from resonance and hence requires higher optical powers. By nanostructuring natural and composite materials it is possible to overcome some of these limitations and move towards realization of devices which are efficient, require low power and are fast. In the context of optical devices fast is actually ultrafast and implies time scales of the order of picoseconds, femtoseonds or less.

However, the current understanding of the physics of the materials and their interactions at nanometer length scales is not sufficient to allow accurate a priori calculation of their properties for designing specific devices. Thus a lot of work is going on to study various properties of nanostructured materials and understand their dependence on the material and structural parameters. Time-resolved nonlinear optical spectroscopy is a powerful tool for studies of energy level structures and carrier dynamics in materials. We are studying the ultrafast optical properties of nanostructures in order to understand and model the effect of structure on the carrier dynamics. This article describes in brief the recent and ongoing activities in this area in our lab.

Why ultrafast?

Any phenomenon occurring with a time scale shorter than a picosecond (10^{-12} s) can be termed ultrafast. On a "microscopic" level everything is ultrafast! The intramolecular atomic motion in molecules and lattice vibrations in solids occur on picosecond timescales. Electron movement in molecules and nanostructures happens at femtosecond time scales (10^{-15} s) whereas the orbital motion of electrons within an atom is even faster [6].

Thus, to understand macroscopic physical phenomena in materials at the fundamental level, ultrafast spectroscopy is required. Even chemical reactions are ultimately governed by the movement of electrons between atoms which can occur on ultrafast time scales. This realization gave birth to the field of femtochemistry and the 1999 Chemistry Nobel prize. Using ultrafast pulses to control a chemical reaction is now a rich field of study [e.g. 7]. Similarly, biological processes also contain a step/steps occurring on an ultrafast time scale. Studies of the mechanism of photosynthesis and vision are the by-now-famous examples of ultrafast processes in biology [8, 9].

Tools of the trade

The light sources for ultrafast spectroscopy are almost always ultrafast lasers. For generating sub-ps pulses the workhorse at the moment are Ti:Sapphire laser based systems although fibre laser based systems are fast catching up. Most ultrafast lasers systems consist of a low energy, high rep-rate oscillator followed by a low rep-rate amplifier. The oscillators exploit the wide tunability of the Ti:S crystal but the amplifiers are designed for operation at a fixed wavelength. Wavelength tuning is then achieved by using an optical parametric amplifier (OPA) after the Ti:S amplifier.

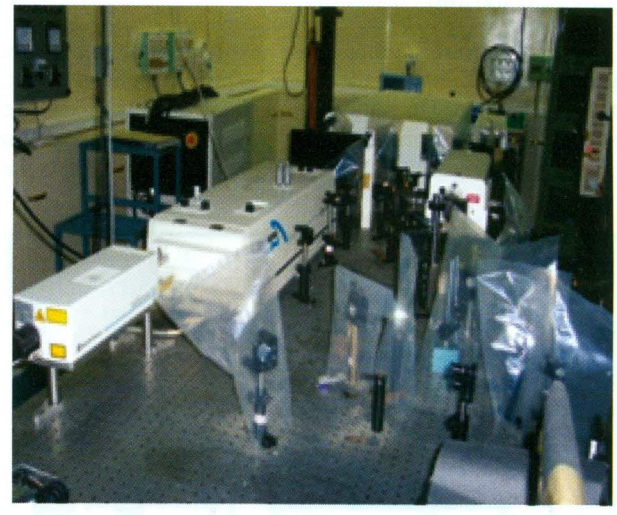

Fig T.2.1. The femtosecond laser system in our lab

The laser system in our lab (Fig.T.2.1) includes a Ti:S laser oscillator with an output of 82 MHz, ~ 10 nJ pulses in the wavelength range 750 -850 nm. This is followed by an amplifier working at 1 KHz, 800 nm. The amplifier pumps an OPA. The output pulse width is typically 100 fs. The system

is arranged so that the output beam from any of the three lasers (oscillator, amplifier or OPA) can be routed to the experiment. These facilities are expected to be augmented soon with new laser systems allowing access to a larger wavelength range and shorter pulses.

Most of the experiments in our lab utilize the pump-probe configuration to extract the fast evolution dynamics of photo-generated carriers. In the basic pump-probe technique the laser pulse is split in two parts of unequal intensity by a beam splitter. The resultant strong pump beam and the weak probe beam are sent along different paths to the sample under study. The time taken for the pulse to reach the sample from the beam splitter is equal to optical path length from beam splitter to sample in meters divided by $3x10^8$. One of the two paths has provision for varying the path length by using an optical delay stage. An optical delay stage consists of a retro reflector mounted on a linear translation stage. Moving this stage along the path of the beam changes the path length travelled by the beam without any lateral spatial shift, i.e. the beam keeps falling on the same area but at different times. Thus the two pulses (pump and probe) can be adjusted to reach the sample either at the same time or with a known time delay between them. The sample response is measured as a function of the delay between the pump and the probe pulses. As can be inferred from the relationship given above, a very small time difference translates into a directly measurable path difference. For example, a 1 ps difference in the arrival of the two pulses at the sample will occur if the two paths differ by 0.3 mm (300 μm).

The strong pump pulse excites photo-generated carriers in the sample under study causing a change in its optical properties. The optical properties can be, for example, absorption, reflection, diffraction or emission from the sample. As long as the pump pulse intensity is below the threshold of the material the optical properties recover to the damage unperturbed state. This recovery is measured by the probe pulses arriving at the sample at different times. Fig.T.2.2 shows the schematic of a few pump-probe configurations. As shown above, an optical delay stage can generate optical delay times of ultrafast accuracy by controlling the linear displacement of the stage with micron-level accuracy. Thus this arrangement allows us to monitor the evolution in optical properties at ultrafast time scales without the necessity of an ultrafast detector. The experiment thus entails movement on the delay stage in incremental steps and at each step measurement of the probe beam after its interaction with the sample. The commonly used translation stages in the optical delays are good quality stepper motor controlled linear stages. Obviously the step size accuracy is a crucial parameter in determining the achievable time resolution. In addition, it is imperative to have wobble-free linear movement with pitch and yaw as small as possible. Otherwise the spatial overlap of the two beams (pump and probe) on the sample would change with the movement of the stage giving rise to a spurious signal. For example, in one of the experiments the transient response of the sample appeared to take a few hundred ps for almost full recovery. This required that the pump-probe delay be varied from zero 800 ps. The baseline (zero level of the signal) is taken to be the signal at negative delay i.e. when the probe pulse precedes the pump pulse on the sample. Thus a total delay scan of ~ 810 ps was required corresponding to a stage movement of a little over 121 mm. The optical path length from the delay stage to the sample is typically 1 m and the beam diameter is ~ 2 mm. A tilt of the stage by 100 rad during its movement would mean a shift of the probe beam spot on the sample by 100 microns. To minimize the error due to this change in overlap we focus the pump and probe beams on the sample such that the probe beam spot size is much less than that of the pump. For this very reason the overall beam pointing stability should be excellent and therefore the lab environment should provide stable ambient conditions. In our lab the temperature is controlled to within 1° C and the experiment is mounted on a curtained vibration isolation table. Still our experience is that the more sensitive measurements are possible only late in the evening or on holidays when human and vehicular traffic in and around the building reduces and other equipments using high power motors in the building are switched off.

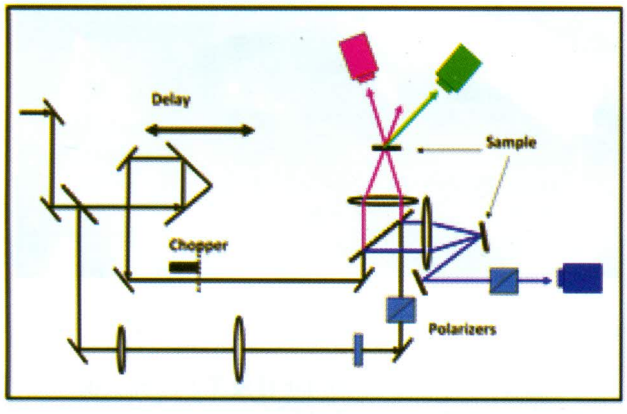

Fig 2. A schematic of a pump-probe experiment showing the transmission (pink), reflection (blue) and diffraction (green) geometries.

It is to be noted that the measurement sensitivity required for these experiments is very high. For example, a reliable measurement of relative change in transmission, T/T, as small as 10^{-5} should be possible. Further, the decay curves are single or multiple exponentials. So a high-fidelity measurement of the decay curve demands that the measurement system have a high dynamic range. This required detection sensitivity is achieved by utilizing phase sensitive detection schemes. One of the beams is power

modulated by introducing a mechanical or optical chopper in the beam path. The signal to be measured is fed to a lock-in amplifier which extracts the component of the signal at the modulation frequency. This allows a high discrimination against wide-band (white) noise.

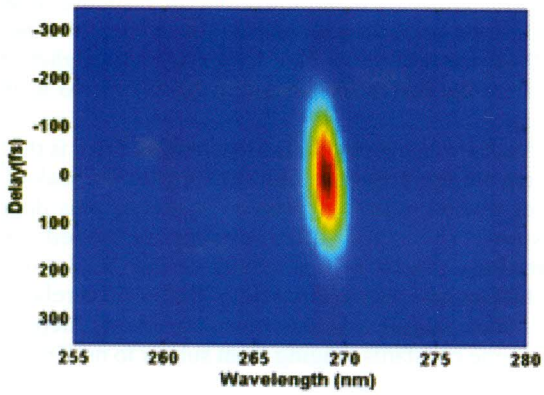

Fig T.2.3. A FROG (frequency resolved optical gating) trace of a UV beam at generated by frequency mixing the laser pulse at 800 nm and its second harmonic at 400 nm in a nonlinear crystal.

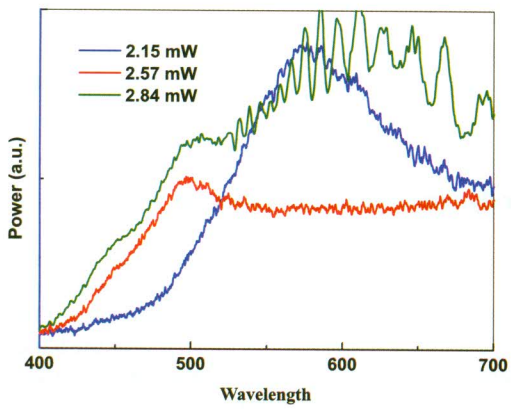

Fig T.2.4. White light continuum spectra generated by focusing a part of the 100 fs, 1 kHz femtosecond amplifier beam in a fused silica disc. The picture shows the dependence of the spectrum characteristics on the input average power. For pump-probe spectroscopy experiments a flat spectrum without modulations is desirable.

Depending on the material under study and the information one is looking for different configurations of the pump-probe technique are used. One variation is to use different wavelengths for the pump and probe. This non-degenerate scheme can be implemented in several ways: (a) by using two synchronized lasers, (b) using two OPA's pumped by the same fs amplifier, (c) generating higher harmonics of one of the beams (Fig T.2.3), (d) generating a white light continuum for the probe by passing the fs laser beam in a Kerr medium (Fig T.2.4) or (e) using a THz transient generated by the fs pulse (Fig T.2.5).

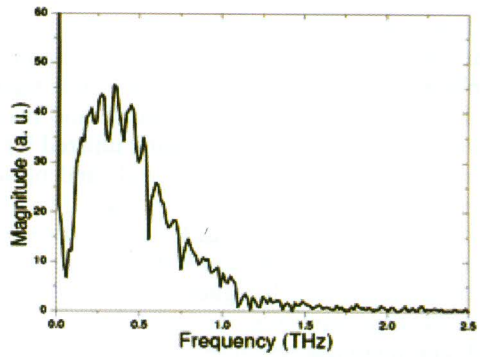

Fig T.2.5. A typical THz transient generated by focusing the 100 fs laser pulses on a photoconductive antenna.

In our lab we use several of these configurations. Fig T.2.6 below shows one such experimental setup in our lab. The stepper motor controlled delay stage is seen in the centre which is in the probe beam path. The pump beam path is in the foreground with a mechanical chopper inserted to modulate the beam for lock-in detection. The unit projecting over the table at the right is an optical cryostat used for temperature dependent studies. To avoid vibrations on the table, the body of the cryostat is mounted on the floor next to the experimental table and only the sample holder chamber with the optical ports is projected on the table.

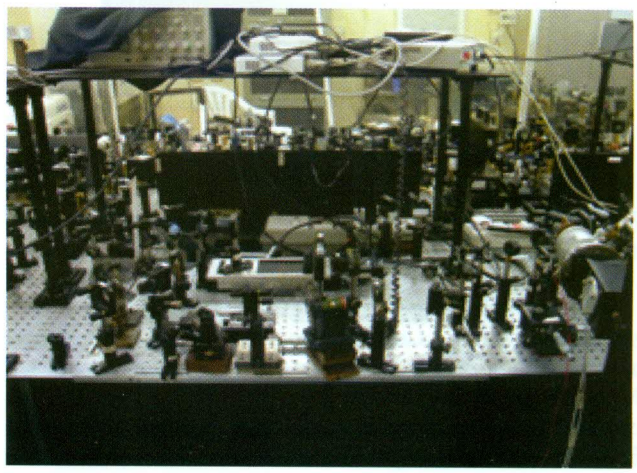

Fig T.2.6. An experimental setup in our lab.

In the following we describe some of our work on carrier dynamics in nanostructures carried out using the above facilities.

Carrier dynamics in silver nanoparticle colloids

Metal nanoparticles possess interesting linear and nonlinear optical properties because they exhibit a local surface plasmon resonance (LSPR) in the visible region. The ability of metallic nanostructures to guide and manipulate light on nanometer length scales is being utilized for several applications in the field of metamaterials and plasmonics. This ability arises from the optical properties of the localized surface plasmon resonances (LSPR) of the free electrons within the nanoparticle. At the LSPR the field strength in and around the particle is much higher than that of the applied field and therefore optically nonlinear behavior is easily observed. This nonlinear response is also fast (ps or less) and therefore the emerging field of nonlinear plasmonics has the potential to speedup computation and communication by directly controlling light with light [11].

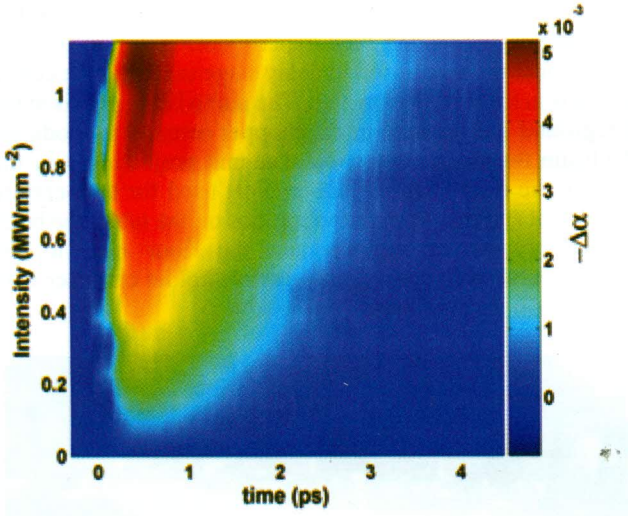

Fig T.2.7. Time-intensity plot of the transient absorption in silver nanoplatelet-water colloids

In nonlinear optical devices the commonly used nonlinear phenomena are the second and third order but there are specific applications utilizing the higher order responses. Measurement of the magnitude of the higher order nonlinear optical response of a material is reasonably well-established. However it is not so easy to determine the time response in the various orders. We demonstrated a new two-dimensional way of analyzing conventional transient absorption data which can be used to determine the magnitude as well as the decay time of the imaginary part of the higher order optical nonlinearities [12-14]. Fig T.2.7 shows a 2-D time-intensity plot of transient absorption measurements on a silver nanoplatelet colloid. The time axis shows the delay between the pump and probe pulses and the intensity axis shows the change in the absorption of the probe pulse in the sample after excitation by the pump pulse. By analyzing various time-slices of this graph we determined that the response times of the third-, fifth- and seventh-order nonlinearity are 0.9 ps, 0.4 ps and 0.3 ps respectively. Thus by going to the higher order nonlinearity the optical response can be made two to three times faster.

Another interesting fact apparent from Fig 7 is that the absorption change peaks at a finite delay after the peak of the 100 fs excitation pulse. A detailed modeling was done to understand the rich information extracted from measurements similar to that shown in Fig T.2.3 [6]. The picture that emerges is the following. The electron relaxation in metal nanoparticle colloids contains several steps with different time constants ranging from sub-ps to ns. Therefore the observed behavior would depend also on the pulse width of the laser used for making the measurements. In case of a 100fs laser pulse the strongest contribution comes due to the thermalization of the high kinetic energy electrons generated by the excitation pulse. This can take a few hundred fs and therefore leads to a delayed but strong nonlinear response in the present case. This work demonstrated that the in metal nanoparticles colloids the "delayed" response at ~ 500 fs is much stronger than the "instantaneous " nonlinear response and thus may be a more efficient regime for fast device operation.

Carrier dynamics in single quantum wells

Another area of our current studies is to study the effect of surface states on carrier dynamics in quantum well structures. For low thickness surface barriers, the QW states can couple with the surface states located near the band edges. This opens an extra channel for the decay of photo-generated carriers. For device applications like photodetectors and modulators this reduction in carrier lifetime can be extremely beneficial. We are currently studying the carrier dynamics in single $GaAs_{0.86}P_{0.14}/Al_{0.7}Ga_{0.3}As$ quantum wells. These are grown at SCLS, RRCAT and are similar to structures used in diode lasers. The quantum well structure is shown in Fig. T.2.8. The initial question that we were trying to answer was what, if any, effect would be seen on the quantum well properties once the top barrier layer is thinned down to 5 nm (sample no. QW5) from 50 nm (sample no. QW50). From calculations and photo-reflectance spectroscopy measurements it appeared that there is no difference in the lowest energy allowed transition (e1 - lh1) in the two quantum well structures. However the photoluminescence (PL)

behavior of the two samples was different and it appeared that the proximity of surface states starts affecting the PL as the top AlGaAs layer is reduced to 5 nm [15]. To resolve this, it was decided to look at the carrier dynamics in the two samples.

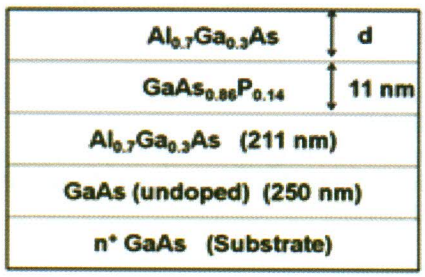

Fig T.2.8.. Schematic of the quantum well structure. The top layer thickness, d, in the two structures under study is 5 nm and 50 nm respectively.

At room temperature, the lowest energy quantum well transitions lie between 770- 790 nm. However the underlying GaAs substrate absorbs completely in this wavelength range and no signal is obtained in transmission. Therefore transient reflectivity geometry was used for this experiment. Fig T.2.9 clearly shows that the decay is different in the two samples. This difference is attributed to one process in the multi-component decay changing sign between the two samples. This is apparently due to the difference in the capping layer thickness. This is being investigated further.

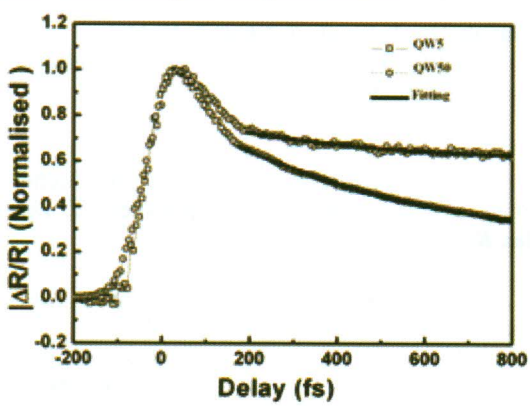

Fig T.2.9. Room temperature transient reflectivity from the two QW samples.

In the sample with the thicker barrier layer, an interesting phenomenon was observed. In the graph shown in Fig T.2.8 the features at very small time delays (< 1 ps) are masked. If this region is expanded and the slow decay is subtracted we see a very fast feature with an oscillatory tail component (Fig T.2.10).

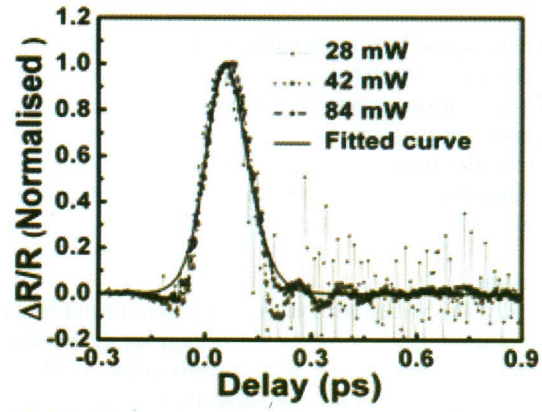

Fig T.2.10. The early part of the transient reflectivity decay for sample QW 50 for different pump powers

This sub-ps component is attributed to thermalization of the photo-generated carriers. However, the oscillatory structure in the tail part is unusual and, to the best of our knowledge, not reported earlier. We recall that the measurements are performed with a femtosecond laser which has a spectral width spanning several optical transitions in the quantum well structure. For example, Fig T.2.11 shows the PL spectrum with the three component transitions as well as the excitation laser spectrum. With the laser spectrum as shown, three transitions, namely e1-hh1, e1–hh2 and e1-lh1, are excited leading to the possibility of a coherent interaction.

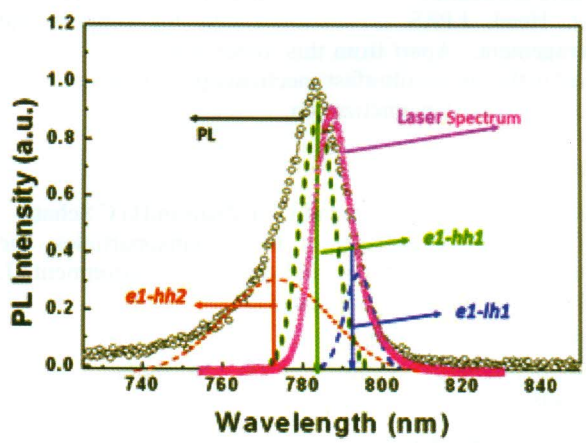

Fig T.2.11. Photoluminescence from QW50 along with the spectrum of the excitation pulse with peak wavelength at 786 nm.

Currently efforts are on to understand and model the carrier dynamics in these structures based on several measurements done in our lab. These include wavelength, temperature and intensity dependent transient reflectivity measurements. One intriguing phenomenon observed an

unexpected signal at wavelengths well below the quantum well transitions. A strong possibility is that the interfaces between the various layers of the sample are playing a role. Subsequent measurements on an AlGaAs/GaAs sample showed similar transient reflectivity features. Therefore we are now investigating the role of this interface in the transient reflectivity of the quantum well structure.

Conclusion

Ultrafast Nanoplasmonics could benefit applications such as computing and information storage on the nanoscale, the ultrasensitive detection and spectroscopy of physical, chemical and biological nanosized objects, and the development of optoelectronic devices. Because of their broad spectral bandwidth, surface plasmons undergo ultrafast dynamics with timescales as short as a few hundred attoseconds. This article describes some of the R&D activity being carried out in the field of ultrafast spectroscopy of nanostructured materials at LPAS, RRCAT. The lab facilities and some recent results have been described. The results shown above are from the work of Dr. J. Jayabalan, Sri Salahuddin Khan and Smt. Asha Singh from LPAS and collaborators from other laboratories in RRCAT. Many of these results have been published/ being published.

Acknowledgement

All the authors/coauthors of the papers from the lab cited here are acknowledged for their contribution. Dr. H. S. Rawat, Head, LPAS is acknowledged for support and encouragement. Apart from this, other activities going on/ planned in the lab are ultrafast spectroscopy of molecules and studies on ultrafast magnetization.

References

1. K. Lance Kelly, E. Coronado, L L Zhao and G C Schatz
The optical properties of metal nanaoparticles: the influence of size, shape and dielectric environment, **J. Phys. Chem. B** 107, 668 (2003)

2. Dieter Bimberg, (Ed)
Semiconductor Nanostructures, Springer , Berlin (2008)

3. J. Jayabalan, M. P. Singh, A. Banerjee and K. C. Rustagi
Linear and nonlinear second-order polarizabilities of hemispherical and sector-shaped metal nanoparticles, **Phys. Rev. B**. 77, 045421 (2008).

4. J. Shah
Ultrafast Spectroscopy of Semiconductors and Semiconductor Nanostructures; Springer: Berlin, 1999.

5. Martin J. A. Schuetz, Michael J. Moore and Carlo Piermarocchi
Trionic optical potential for electrons in semiconductors, Nature Physics, 6, 919 (2010)

6. X. Xie, S. Roither, D. Kartashov, E. Persson, D. Arbó, Li Zhang, S. Gräfe, M. Schöffler, J. Burgdörfer, A. Baltuška, M. Kitzler.
Attosecond Probe of Valence-Electron Wave Packets by Subcycle Sculpted Laser Fields. **Physical Review Letters**, 108 (19) (2012)

7. Paul Hockett, Christer Z. Bisgaard, Owen J. Clarkin and Albert Stolwo
Time-resolved imaging of purely valence-electron dynamics during a chemical reaction, **Nature Physics**, 1, 17Apr (2011)

8. W. Zinth, J. Wachtveiti
The first picoseconds in bacterial photosynthesis--ultrafast electron transfer for the efficient conversion of light energy
Chemphyschem, 6(5), 871 (2005)

9. Qing Wang, Robert W. Schoenlein, Linda A. Peteanu, Richard A. Mathies, Charles, W. Shank
Vibrationary coherent photochemistry in the femtosecond primary event of vision, **Science, 266,** 422(1994)

10. Shradha Palod, R. Chari, S.M. Oak, A. G. Bhujle
Automation of Pump Probe Experiments with Data Acquisition, Control and Analysis, CAT 2005-05

11. J. Jayabalan, A. Singh, R. Chari, S.M. Oak
Nonlinearity of silver nanospheres and nanodiscs, Nanotechnology 18, 315704 (2007)

12. J. Jayabalan
Origin and the time dependence of higher-order nonlinearities in metal nanocomposites,, ***J. Opt. Soc. Am. B***, 28, 2448-2455 (2011)

13. J. Jayabalan, Asha Singh, Rama Chari, Salahuddin Khan, Himanshu Srivastava, and S. M. Oak,
Transient Absorption and Higher-order Nonlinearities in Silver Nanoplatelets, **App. Phys. Lett**., 94, 181902 (2009).

14. J. Jaybalan, A. Singh, S. Khan, R. Chari
Third-order nonlinearity of metal nanoparticles: Isolation of instantaneous and delayed contributions, **J. Appl. Phys**. 112, 103524 (2012)

15. S. Pal, S.D. Singh, S. Porwal, T.K. Sharma, S. Khan, J. Jayabalan, R. Chari, S. M. Oak,
Effect of light hole tunneling on the excitonic properties of GaAsP/ AlGaAs ner-surface quantum wells, Semicond. Sc. Tech. (accepted)